IEEE Photonics Journal
An IEEE Photonics Society Publication

Open Access

Joint Time and Frequency Dissemination Network Over Delay-Stabilized Fiber Optic Links

Volume 7, Number 3, June 2015

Wei Chen
Qin Liu
Nan Cheng
Dan Xu
Fei Yang
Youzhen Gui
Haiwen Cai

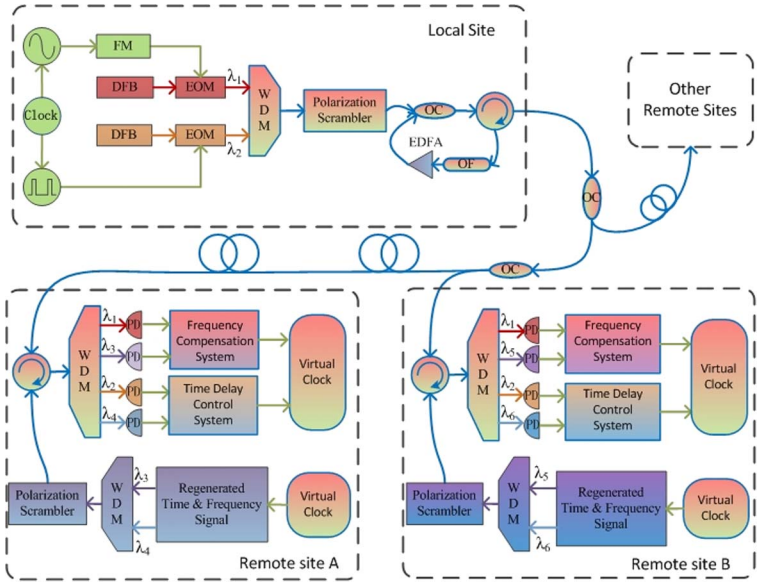

DOI: 10.1109/JPHOT.2015.2426874
1943-0655

Joint Time and Frequency Dissemination Network Over Delay-Stabilized Fiber Optic Links

Wei Chen,[1,2] Qin Liu,[2,3] Nan Cheng,[1,2] Dan Xu,[1,2] Fei Yang,[1] Youzhen Gui,[3] and Haiwen Cai[1]

[1]Shanghai Key Laboratory of All Solid-State Laser and Applied Techniques, Shanghai Institute of Optics and Fine Mechanics, Chinese Academy of Sciences, Shanghai 201800, China
[2]Graduate University of the Chinese Academy of Sciences, Beijing 100049, China
[3]Key Laboratory for Quantum Optics, Shanghai Institute of Optics and Fine Mechanics, Chinese Academy of Sciences, Shanghai 201800, China

DOI: 10.1109/JPHOT.2015.2426874

Manuscript received April 6, 2015; accepted April 20, 2015. Date of publication April 28, 2015; date of current version May 13, 2015. This work was supported in part by the National Natural Science Foundation of China under Grant 61405227. Corresponding authors: Y. Z. Gui and H. W. Cai (e-mail: yzgui@siom.ac.cn; hwcai@siom.ac.cn).

Abstract: A precise fiber-based time and frequency dissemination scheme for multiple users with a tree-like branching topology is proposed. Through this scheme, ultrastable signals can be easily accessed online without affecting other sites. The scheme is tested through an experiment, in which a modulated frequency signal and a synchronized time signal are transferred to multiple remote sites over delay-stabilized fiber optic links that are over 50 km long. Results show that the relative stabilities are 5×10^{-14} at 1 s and 2×10^{-17} at 10^4 s. Meanwhile, compared with each site, time synchronization precision is less than 80 ps. These results can pave the way to practical applications in joint time and frequency dissemination network systems.

Index Terms: Fiber optics systems, time and frequency transfer, fiber optics network, frequency stability.

1. Introduction

Fiber-based frequency peer-to-peer transfer has been widely discussed and developed with the progress of atomic clocks, wherein Global Positioning System methods are insufficient for short-term performance of a microwave or an optical frequency standard [1]–[3]. Moreover, to extend the range of practical applications, in recent years, considerable interest has been focused on frequency dissemination to multiple users via fiber optic [4]–[7], which is a challenging task in using a simple control system and an optimized topological cyber structure. As a linear topology, midpoint extraction in a trunk fiber for multiple accesses has been first proposed to address this problem [4]–[6]. Meanwhile, another tree-like topology, wherein an optical frequency is disseminated to two sites by the multiple reflections compensation method, is also effective [7]. Both schemes produce good results in radio or optical frequency dissemination. To our knowledge, the frequency instability is better than 7×10^{-14} at 1 s for radio frequency and 8×10^{-16} at 1 s for optical frequency in the access node [5], [8].

However, many applications such as modern large linear accelerators, very long base line interferometry (VLBI), and deep space networks (DSN) are inclined to have synchronized time

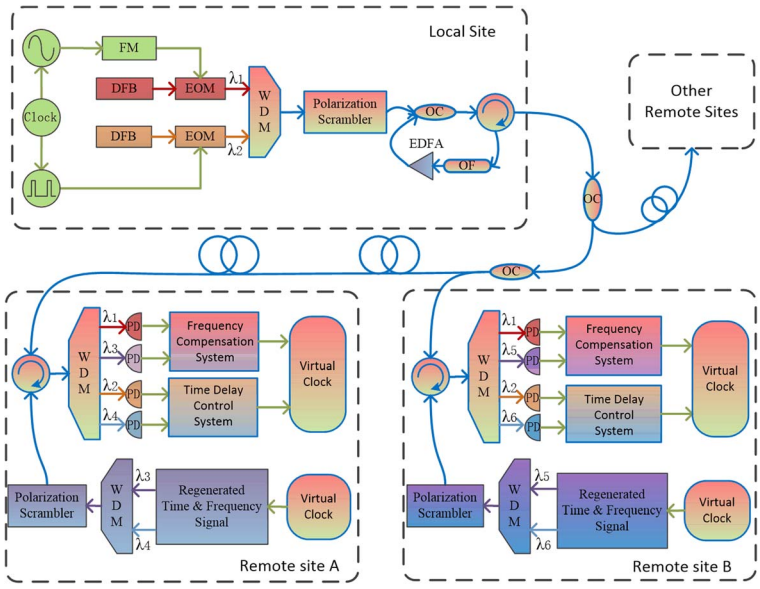

Fig. 1. Schematic of the dissemination structure. DFB: distributed feedback laser, EOM: electro-optic modulator, WDM: wavelength division multiplexer, OC: optical coupler, OF: optical filter, EDFA: erbium-doped fiber amplifier, PD: photodetector, FM: frequency multiplier.

with ultra-stable frequency at different remote sites [9]–[12]. All the aforementioned applications need to determine the exact delay time between each terminal for precise synchronization and to simultaneously access a stable frequency signal to reduce timing uncertainty over free-running time [13]. Consequently, in this study, we propose a scheme to transfer time and frequency jointly to multiple users through a tree-like fiber network with a noise compensation system at each remote site, which will highly reduce system complexity at the local station. Through this scheme, all terminals can be time and frequency synchronized via a delay-stabilized fiber optic link. Relative stabilities of 5×10^{-14} at 1 s and 2×10^{-17} at 10^4 s are obtained while the time synchronization precision of 80 ps is reached.

This paper is organized as follows. The outline of the joint time and frequency dissemination scheme, which exhibits a noise compensation strategy, is first described. Afterward, detailed theories on phase compensation and time synchronization are derived. Then, an experiment is demonstrated and the results of relative frequency stability and synchronization performance are shown by calculating the phase drifting and comparing the absolute time of different sites. Subsequently, some residual factors that may affect the capacity of a network system are discussed. Finally, a conclusion of this study is provided and potential applications are presented.

2. Experimental Scheme

The proposed scheme is illustrated in Fig. 1. The local site has a simple structure. No additional components are required and new remote sites can be inserted in the future. The 10 MHz frequency signal from a high-precision clock is multiplied to a higher frequency for the distributed feedback (DFB) laser, which has a considerably lower intensity noise at higher frequency levels that results in higher signal-to-noise ratio (SNR) for compensation [13], [14]. Meanwhile, the one pulse per second (1 PPS) time signal is produced by a time generator and locked by the same clock. Dense wavelength division multiplexing technology is applied to multiplex time and frequency signals. Light from two externally modulated lasers with different wavelengths ($\lambda_1 = 1548.5$ nm and $\lambda_2 = 1549.3$ nm) are transferred to polarization scrambler after multiplexing through the same fiber link. The polarization scrambler can reduce the polarization effect such as polarization mode dispersion [15]. Before being injected into the long-haul fiber, signals

pass through a back-and-forth control structure that consists of an optical coupler (OC), a circulator, an optical filter (OF), and an erbium-doped fiber amplifier (EDFA). This structure is used to pass the forward signal while amplifying and reflecting the backward signal. Here, we use a customized dense wavelength division multiplexer (DWDM) as a band stop optical filter with a stop bandwidth of 100 GHz. It is designed to pass light in the optical C waveband expect for the wavelengths λ_1 and λ_2. This suppresses backscattering of the forward signals injected into the EDFA, and improves the system noise performance. In addition, we increase the length of the filter to reduce backscattered light from the reflected ("backward") signal in the forward direction coming into the EDFA as well as increase the fiber length between the coupler and circulator to keep the control structure symmetric. Any asymmetry in the fiber length of the back-and-forth structure is less than 0.1 m and the whole structure on which we do not have active temperature control is put into a case with a temperature stability of about ± 1 °C. Using a thermal sensitivity of 36.8 ps/(km · K) [16], the corresponding instability level is about 7.4 fs. Thus temporal drift due to an asymmetric path can be neglected. After passing through the back-and-forth structure, the joint time and frequency signals along the fiber link can be extracted by an OC, just like in a tree-like network.

At each remote site, time and frequency signals are detected and recovered by two low-noise photodetectors after they are demultiplexed by a four-channel wavelength division multiplexer (WDM). Subsequently, the frequency and time signals are sent to the phase noise compensation system and the time delay control system, respectively. Because of the advantages of the optical fiber link, the short term performance of these two signals is good even though the phase fluctuations are not compensated. Therefore, the recovered signal can be regarded as a virtual clock whose signals have an acceptable short-term stability. In fact, as long as the induced short-term instability of the dissemination system is lower than the instability of the atomic clock itself (usually about $1e^{-12}$ at 1 s for a commercial Cesium clock), the recovered signal can be viewed as acceptable. Now that a virtual clock is obtained, the basic concept of the noise compensation method can be applied as the traditional round trip method [16]–[18] at a remote site. In our scheme, two additional wavelength lasers ($\lambda_3 = 1547.7$ nm and $\lambda_4 = 1550.1$ nm for remote site A while $\lambda_5 = 1546.9$ nm and $\lambda_6 = 1550.9$ nm for remote site B), which are regarded as sensing signals modulated by the regenerated time and frequency signals, are sent back to the local site. After passing through the back-and-forth structure, the sensing signals move along the original path and are demultiplexed by the other two channels of the four-channel WDM at a remote site. Hence, the additional phase noise and time delay induced by the transmitted fiber are detected by sensing signals. They can be respectively compensated by the phase noise compensation and time delay control systems.

For additional details, we first focus on the frequency signal, as shown schematically in Fig. 2(a). As previously discussed, the 10 MHz frequency signal V_r is boosted to a 1 GHz signal $V_0 = \cos(\omega t + \varphi_0)$ without considering its amplitude. Then, the intensity of the DFB laser with wavelength of 1548.5 nm (marked as λ_1) is modulated by an electro-optic Mach–Zehnder modulator. After multiplexing with the time signal, the frequency signal is injected into the long-haul fiber link. At the remote terminal (here we use remote site A as an example, but the same process applies to other remote sites), the frequency signal coming from a local site first passes through an optical delay line (ODL), including a temperature controlled fiber optic ring (with sensitivity of 40 ps/°C for a 1 km temperature controlled ring and 350 ps/°C for a 10 km temperature controlled ring, noting that the sensitivity decreases with increasing length of the delay fiber due to a less uniform heating of the fiber on the spool) and a fast fiber stretcher (response speed of a few hundreds kHz) as a compensated structure. Detected by a low-noise photodetector, the frequency signal with one-trip phase fluctuation $\Delta\varphi_p$ can be expressed as $V_{a1} = \cos(\omega t + \varphi_0 + \varphi_L + \varphi_{ODL} + \Delta\varphi_p)$, where φ_L and φ_{ODL} are the inherent phase shift term of the fiber link and ODL respectively and they are regarded as constant. It splits into three parts. In the first part, the output frequency signal whose phase will be stabilized is down converted to 10 MHz as the final signal output. In the second part, the signal is sent to the phase discriminator as reference. In the third part, V_{a1}, as a sensing signal, modulates another DFB laser with a

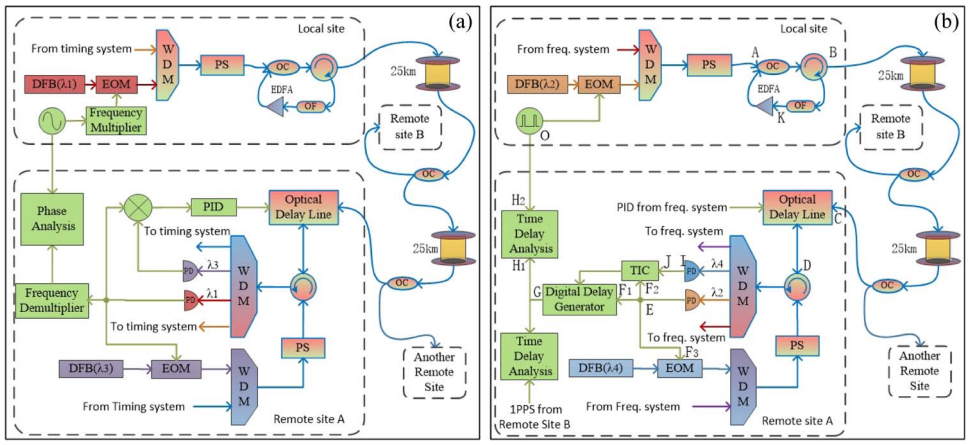

Fig. 2. Outlines of the compensation system for time and frequency dissemination for (a) phase noise compensation and (b) time delay synchronization. DFB: distributed feedback laser, EOM: electron optic modulator, WDM: wavelength division multiplexer, PS: polarization scrambler, OC: optical coupler, OF: optical filter, EDFA: erbium-doped fiber amplifier, PID: proportional-integral-derivative, PD: photodetector, TIC: time interval counter.

1547.7 nm wavelength (marked as λ_3). Because the length of the long-haul fiber spools (50 km for site A and 25 km for site B) are much longer than that of some asymmetric parts, like the back-and-forth control structure, the optical path is assumed to be symmetric. Hence, when the sensing frequency signal returns to the remote site, the detected signal after demultiplexing with the corresponding channel becomes $V_{a3} = \cos(\omega t + \varphi_0 + 3\varphi_L + 3\varphi_{ODL} + 3\Delta\varphi_p)$, which is also sent to the phase discriminator. Therefore, the beat note signal, which is proportional to $2\varphi_L + 2\varphi_{ODL} + 2\Delta\varphi_p$, is obtained. After the proportional-integral-derivative arithmetic is applied, an error signal of $-\Delta\varphi_p$ is sent as feedback to the ODL for compensation. The phase shift of the ODL changes to $\varphi'_{ODL} = \varphi_{ODL} - \Delta\varphi_p$. Now, the output frequency is stabilized to $V'_{a1} = \cos(\omega t + \varphi_0 + \varphi_L + \varphi'_{ODL} + \Delta\varphi_p) = \cos(\omega t + \varphi_0 + \varphi_{L+}\varphi_{ODL})$. At last it is down converted to 10 MHz for users. Thus, the stable frequency is obtained.

Similarly, Fig. 2(b) outlines the principle of the time synchronization system that we have developed. For the time signal, the local site is the same with the frequency signal but modulating another DFB laser with wavelength of 1549.3 nm (marked as λ_2). Because the time and frequency carriers go through the same fiber path, the impact of vibration, temperature and humidity on the fiber is almost the same for the two signals. Thus, when the 1 PPS signal pass the ODL at each remote site, its phase will be stabilized accompany with the frequency signal. Then, the 1 PPS signal is detected and split into three parts at point E. In the first part, the digital delay generator is triggered. In the second part, the signal is sent to the time interval counter (TIC) as the counting start time. In the third part, the signal is used to modulate another DFB laser with wavelength of 1550.1 nm (marked as λ_4) that still has a 100 GHz space with the local one. When this light returns to the local site and is resend to the remote site once again, it is detected and sent to the TIC as the counting stop time. The counting time controls the digital delay generator to compensate time delay after calculation. Although the optical path cannot be absolutely symmetrical, particularly at remote sites, all the terminals can still be synchronized after some calibration. That is, the time signal of the remote terminal output (point G) can be always synchronized with the local clock (point O) using the proposed dissemination scheme.

For easy calibration, some cables are selected to have the same length such as $L_{EF1} = L_{EF2} = L_{EF3}$ and $L_{OH2} = L_{GH1}$, and some detail effects like the stability of the wavelengths of the DFB laser, thermo-stability of the components of the instrument are carefully controlled but not further discussed here. The intrinsic delay of the system for our synchronization scheme is calibrated in two steps. The calibration is processed in the same ambient temperature. In step one, a back-to-back test is performed, in which the local terminal and remote terminal are positioned

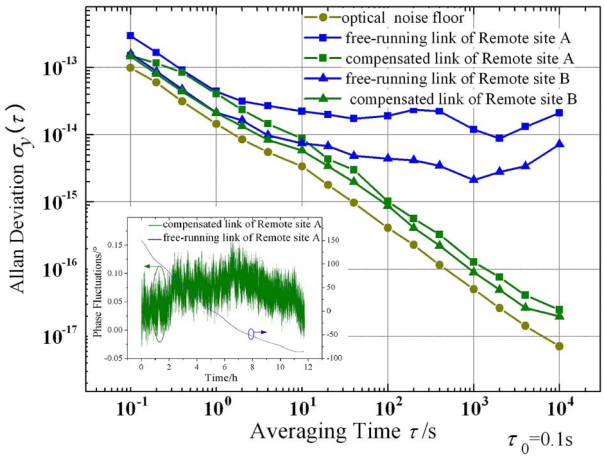

Fig. 3. ADEV of frequency signals at the two remote sites with and without compensation. (Inset) Phase fluctuations of Remote site A with and without compensation.

together without inserting any long-haul fiber link ($t_{BC} = 0$). We need to set a controlled delay time t_{CDT}($t_{CDT} = t_{F1G}$ in Fig. 2, controlled by digital delay generator) to ensure remote end synchronization; thus, we obtain

$$t_{OA} + t_{AB} + t_{CD} + t_{DE} + t_{EF_1} + t_{CDT} = 1 \text{ s}. \tag{1}$$

Then, the TIC display is as follows:

$$t_{TIC} = t_{F_3D} + t_{DC} + t_{BKA} + t_{AB} + t_{CD} + t_{DI} + t_{IJ}. \tag{2}$$

In the second step, the long-haul fiber is placed between two sites, and thus, the TIC display is changed to

$$t_{TIC'} = t_{F_3D} + t_{DC} + t_{CB} + t_{BA} + t_{AB} + t_{BC} + t_{CD} + t_{DI} + t_{IJ} \tag{3}$$

where t_{CB} and t_{BC} are the fiber propagation delays in both directions. The propagation delays along the long-haul fiber in both directions are assumed to be equal and equally change with ambient temperature. Thus, compared with those in (2) and (3), the asymmetrical path is dramatically canceled. Propagation delay time is simply expressed as follows:

$$t_{BC} = \frac{(t_{TIC'} - t_{TIC})}{2}. \tag{4}$$

In this status, if the 1 PPS signal is synchronized, then another controlled delay time $t_{CDT'}$ will be set. Thus, total delay time is satisfied with the following equation:

$$t_{OA} + t_{AB} + t_{BC} + t_{CD} + t_{DE} + t_{EF_1} + t_{CDT'} = 1 \text{ s}. \tag{5}$$

Using (1) and (4), the controlled delay time is expressed as follows:

$$t_{CDT'} = t_{CDT} - (t_{TIC'} - t_{TIC})/2 \tag{6}$$

which is used to control the digital delay generator. As a matter of fact, the wavelength with a 100 GHz spacing between the back-and-forth light makes the propagation delay time of the two directions different. The effect of chromatic dispersion must be considered, particularly in some long-haul circumstances [19].

3. Experimental Results

As shown in Fig. 2, the link from local to Remote site A is 50 km and local to Remote site B is 25 km, where the two remote sites sharing the same 25 km spool. Meanwhile, a 10 km

temperature controlled delay line and a 20 m fiber stretcher are deployed for Remote site A, while a 1 km temperature controlled delay line and another 20 m stretcher are deployed for Remote site B as compensation structure. The actual link distances from local to the two sites are approximately 60 km and 26 km, respectively. For demonstration, we measure the relative frequency stability of both remote end signals V_a and V_b compared with the frequency reference V_r (with a 5 Hz measurement bandwidth), where both remote sites are located within the same laboratory. The results of the overlapping Allan deviation (ADEV) are shown in Fig. 3. Short-time instability can reach 2×10^{-14} at 1 s and 5×10^{-14} at 1 s, respectively, whereas long-time performance can extend to the 10^{-17} level at an average time of 10^4 s. The free-running behaviors of the two sites are similar because they share the same 25 km fiber spool in the same laboratory. Regardless of the remote site, short-time frequency stability does not improve much while the compensation servo is engaged because of the limitations placed by the relative intensity noise of the active device and the frequency noise of the laser carrier. The optical noise floor is also shown in the figure. Nevertheless, the long-term effect of temperature changes is dramatically suppressed.

The inset in Fig. 3 shows the phase fluctuations over a 12-hour period for a free-running and stabilized link of Remote site A. Note that these phase fluctuations are due to variations in temperature, humidity, mechanical stability, etc. Phase fluctuation is less than about 0.15 degree for the stabilized link, while the phase of the free-running link drifts away by approximately 250 degrees over this time interval, which clearly demonstrates the effect of the compensation system. A small oscillation with time seems to be present in the phase fluctuations for the stabilized link. Two factors should be considered. Phase fluctuations with respect to temperature vary at different wavelengths, and some optical paths are outside the compensation loop. Given that the thermal coefficients of the dispersion is small, i.e. approximately 1.6 $\mathrm{fs}/(\mathrm{nm} \cdot \mathrm{km} \cdot \mathrm{K})$ [20], and the fiber that is outside the loop can be carefully temperature controlled and set as short as possible (such as in our experiment the fiber outside the loop is about 1 m and with temperature turbulence within ± 2 °C), the two factors will not affect practical applications.

The exact propagation delay is obtained after two calibration steps. To achieve a more precise calibration, we measure the chromatic dispersion of the two fiber spools using a dispersion analysis machine (MTS-8000-ODM, JDSU, dispersion uncertainty of ± 0.06 $\mathrm{ps}/\mathrm{nm} \cdot \mathrm{km}$), which shows that the discrimination of the delay time caused by the dispersion are 836.8 ps/nm and 417.3 ps/nm for Remote sites A and B, respectively, at 1550 nm. Consequently, the propagation delay is revised for synchronization. Hence, fiber length variation is stabilized by the phase noise compensation system and the 1 PPS signal is synchronized after calibration. We use a standard time interval counter (SR620) to compare the absolute delay time of three sets of data: local time with Remote site A, local time with Remote site B, and the delay time between these two remote sites. All of the tests are measured for 12 hours. The improvement between free-running and compensation links can be observed in corresponding time deviation (TDEV) plots shown in Fig. 4. We observe that the TDEV of both compensated links decrease to less than 1.8 ps for the average time between $10^2 - 10^4$ s, but they increase if the links are free running. The performance of the synchronization system is illustrated in Fig. 5. All signals are nearly stable along time. The time jitter of the 1 PPS signal, which is measured in 10 s intervals, is approximately 7.5 ps (root mean square). The absolute delay time between different sites are 71, 43, and 20 ps. Notably, the time difference between the remote sites is less than the theoretical subtraction of the local site with Remote site A and the local site with Remote site B because of some measurement errors of the TIC. Even so, all remote sites exhibit good synchronization precision that can satisfy the requirements of essentially most practical applications at present.

4. Discussion

The network capacity of the joint time and frequency dissemination scheme is limited by two considerable factors. First, the optical power budget should cover the additional optical loss caused by network node insertion. For the entire network design, the splitting ratio of the OC

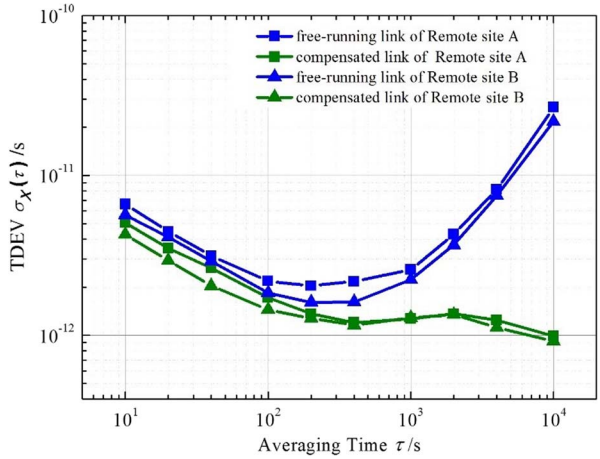

Fig. 4. TEDV of time signals at the two remote sites with and without compensation.

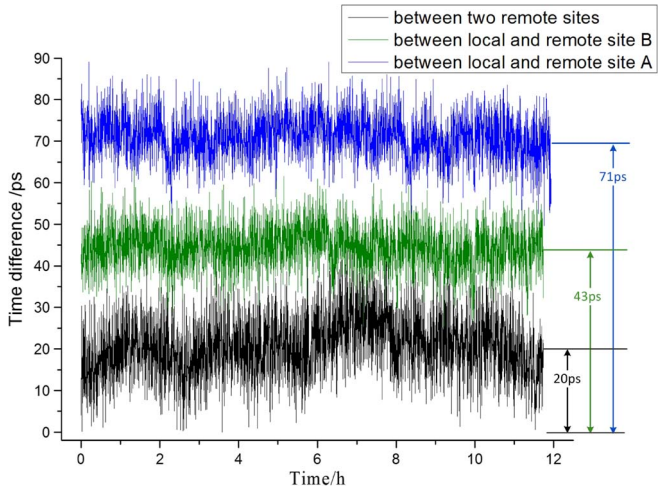

Fig. 5. Time difference between the three sites. Measurements were obtained in 10 s intervals.

should be assigned according to node distance. Bi-EDFA with high symmetry and low amplified spontaneous emission noise can be inserted into the backbone fiber before the OC [21]. This procedure will provide sufficient optical power. Thus, additional optical loss can be addressed. Second, wavelength assignment determines the number of the remote terminals in the scheme. By contrast, different wavelengths are designed for each sensing signal to distinguish each remote site. The advantage of this setup is that remote sites will not affect one another. New terminals can be flexibly inserted, even when other terminals are operating. This experiment has been demonstrated and will be analyzed in the future. However, it limits the capacity in one single fiber. We use waveband C (1525 nm to 1565 nm) as an example. With one backbone fiber, this waveband can only accommodate approximately 25 terminals for a communication channel space of 100 GHz. If there are more remote terminals, the so-called cascaded method can be combined with this scheme [22], [23]. Furthermore, as the number of terminals increases, large dispersion induced by different wavelengths will affect the performance leading to limit the network capacity. Calculating the derivative of fiber propagation delay $\tau = Ln/c$, where L is the length of fiber optic link, n is the refractive index, and c is the speed of light in vacuum, we can get

$$d\tau = \frac{n}{c}dL + \frac{L}{c}dn = \frac{n}{c}\frac{\partial L}{\partial T}dT + \frac{L}{c}\frac{\partial n}{\partial T}dT + \frac{L}{c}\frac{\partial n}{\partial \lambda}d\lambda \tag{7}$$

where T is the temperature of the optical fiber, and λ is the wavelength of the DFB laser. The first two terms in the right side can be suppressed by the compensation system. We focus on the last term in the right side which can be viewed as the chromatic dispersion effect. So the delay deviation induced by the dispersion effect can be expressed as

$$\Delta\tau = LD\Delta\lambda \tag{8}$$

where $D = (\partial n/\partial\lambda)/c$ (usually 17 ps/nm/km) is the fiber dispersion coefficient. It impacts on the time signal. The difference of absolute time delay between back and forth light can be approximately 340 ps/km (for using 1545 nm in the local site and 1525 nm or 1565 nm in the remote site). This part of asymmetry is the dominant factor and will affect the calibration procedure. However, thanks to several dispersion compensation methods can be applied [24], [25] and the value of dispersion can be measured by the dispersion analysis machine, it will not significantly affect time synchronization performance. Further, the dispersion varies with temperature. Taking the partial derivatives of (8), the thermal sensitivity of the delay deviation with respect to dispersion can be expressed as

$$\frac{\partial(\Delta\tau)}{\partial T} = D\frac{\partial L}{\partial T}\Delta\lambda + L\frac{\partial D}{\partial T}\Delta\lambda \tag{9}$$

which leads to the uncertainty for the compensation system and results in the jitter of time and frequency signals. Now this effect can reach 32 $\mathrm{fs}/(\mathrm{km}\cdot\mathrm{K})$ [20] (still using 1545 nm in the local site and 1525 nm or 1565 nm in the remote site to estimate). It is still three orders smaller than the thermal sensitivity of the fiber propagation delay. That is to say, for network capacity design some detail effects as we illustrated should be considered but the dissemination scheme is sufficient for most practical time and frequency dissemination network applications.

5. Conclusion

In this study, we propose a scheme to jointly disseminate time and frequency signals to multiple users using an active stabilization and synchronization system. Compared with existing approaches, the proposed scheme satisfies more actual demands and provides a more flexible and robust online insertion of new remote nodes. Moreover, we perform an experiment to examine the performance of the scheme using a trial link of two 25 km long fiber spools in the laboratory. A time deviation of 1.8 ps at 10^2 s (for time signals) and Allan deviation of 5×10^{-14} at 1 s and 2×10^{-17} at 10^4 s (for frequency signals) are obtained, which prove that the scheme is effective. Some contributive factors that may affect system performance are also discussed in this paper. The solutions to these factors will be tested in the next research. Furthermore, the proposed structure can be extended to a branch networking system for fiber-based time and frequency transfer, even at a continental scale.

Acknowledgment

We would like to thank Prof. Z. J. Fang for helpful discussions and guidance.

References

[1] Y. Y. Jiang *et al.*, "Making optical atomic clocks more stable with 10(-16)-level laser stabilization," *Nat. Photon.*, vol. 5, no. 3, pp. 158–161, Jan. 2011
[2] S. M. Foreman, K. W. Holman, D. D. Hudson, D. J. Jones, and J. Ye, "Remote transfer of ultrastable frequency references via fiber networks," *Rev. Sci. Instrum.*, vol. 78, no. 2, Feb. 2007, Art. ID. 021101.
[3] W. Tseng, S. Lin, K. Feng, M. Fujieda, and H. Maeno, "Improving TWSTFT short-term stability by network time transfer," *IEEE Trans. Ultrason., Ferroelectr., Freq. Control*, vol. 57, no. 1, pp. 161–167, Jan. 2010.
[4] G. Grosche, "Method for making available a reference frequency," German Patent Appl. DE 10.2008.062.139, 2010.
[5] C. Gao *et al.*, "Fiber-based multiple-access ultrastable frequency dissemination," *Opt. Lett.*, vol. 37, no. 22, pp. 4690–4692, Nov. 2012.
[6] Ł. Sliwczynski, P. Krehlik, Ł. Buczek, and M. Lipinski. "Multipoint dissemination of RF frequency in delay-stabilized fiber optic link in a side-branch configuration," in *Proc. Joint UFFC, EFTF PFM Symp.*, Jul. 2013, pp. 876–878.

[7] S. W. Schediwy *et al.*, "High-precision optical frequency dissemination on branching optical-fiber networks," *Opt. Lett.* vol. 38, no. 15, pp. 2893–2896, Jul. 2013.
[8] A. Bercy *et al.*, "In-line extraction of an ultrastable frequency signal over an optical fiber link," *J. Opt. Soc. Amer. B, Opt. Phys.*, vol. 31, no. 4, pp. 678–685, Mar. 2014.
[9] M. Calhoun, S. Huang, and R. L. Tjoelker, "Stable photonic links for frequency and time transfer in the deep-space network and antenna arrays," *Proc. IEEE*, vol. 95, no. 10, pp. 1931–1946, Oct. 2007.
[10] D. Piester, A. Bauch, and L. Breakiron, "Time transfer with nanosecond accuracy for the realization of international atomic time," *Metrologia*, vol. 45, no. 2, pp. 185–198, Apr. 2008.
[11] R. A. Lerche, G. W. Coutts, and L. J. Lagin, "The NIF integrated timing system design and performance," in *Proc. Int. Conf. Accelerators Large Exp. Phys. Control Syst.*, Nov. 2001, pp. 27–33.
[12] D. S. Robertson, "Geophysical applications of very-long-baseline interfereometry," *Rev. Mod. Phys.*, vol. 63, no. 4, pp. 899–918, Oct. 1991.
[13] B. Wang *et al.*, "Precise and continuous time and frequency synchronisation at the 5×10^{-19} accuracy level," *Sci. Rep.*, vol. 2, no. 556, pp. 1–5, Aug. 2012.
[14] O. Lopez, A. Amy-Klein, M. Lours, C. Chardonnet, and G. Santarelli, "High-resolution microwave frequency dissemination on an 86-km urban optical link," *Appl. Phys. B-Lasers O*, vol. 98, no. 4, pp. 723–727, Mar. 2010.
[15] O. Lopez *et al.*, "86-km optical link with a resolution of 2×10^{-18} for RF frequency transfer," *Eur. Phys. J. D*, vol. 48, no. 1, pp. 35–41, Jun. 2008.
[16] Ł. Śliwczyński, P. Krehlik, and M. Lipiński, "Optical fibers in time and frequency transfer," *Meas. Sci. Technol.*, vol. 21, no. 7, May 2010, Art. ID. 075302.
[17] M. Musha, F. L. Hong, K. Nakagawa, and K. Ueda, "Coherent optical frequency transfer over 50-km physical distance using a 120-km-long installed telecom fiber network," *Opt. Exp.*, vol. 16, no. 21, pp. 16 459–16 466, Oct. 2008.
[18] F. Yang, D. Xu, Q. Liu, N. Cheng, Y. Z. Gui, and H. Cai, "Accurate transmission of time and frequency signals over optical fibers based on WDM and two way optical compensation techniques," presented at the CLEO: Science and Innovations Conf., San Jose, CA, USA, JTu4A.99, 2013.
[19] P. Krehlik, Ł. Śliwczyński, Łukaszbuczek, and M. Lipiński, "Fiber-optic joint time and frequency transfer with active stabilization of the propagation delay," *IEEE T. Instrum. Meas.*, vol. 61, no. 10, pp. 2844–2851, Oct. 2012.
[20] S. C. Ebenhag, P. O. Hedekvist, and K. Jaldehag, "Active detection of propagation delay variations in single way time transfer utilizing dual wavelengths in an optical fiber network," in *Proc. Joint Conf. IEEE Int. Frequency Control Eur. Frequency Time Forum*, San Francisco, CA, USA, May 2011, pp. 1–6.
[21] M. Amemiya *et al.*, "Precise frequency comparison system using bidirectional optical amplifiers," *IEEE Trans. Instrum. Meas.*, vol. 59, no. 3, pp. 632–640, Mar. 2010.
[22] M. Fujieda, M. Kumagai, and S. Nagano, "Coherent microwave transfer over a 204-km telecom fiber link by a cascaded system," *IEEE Trans. Ultrason., Ferroelectr., Freq. Control*, vol. 57, no. 1, pp. 168–174, Jan. 2010.
[23] O. Lopez *et al.*, "Cascaded multiplexed optical link on a telecommunication network for frequency dissemination," *Opt. Exp.*, vol. 18, no. 16, pp. 16 849–16 857, Jul. 2010.
[24] L. H. Han *et al.*, "Dispersion compensation properties of dual-concentric core photonic crystal fibers," *Chin. Opt. Lett.*, vol. 12, no. 01, Jan. 2014, Art. ID. 010603.
[25] W. B. Liang, N. L. Liu, Z. H. Li, and P. X. Lu, "Octagonal dual-concentric-core photonic crystal fiber for C-band dispersion compensation with low confinement loss," *Chin. Opt. Lett.*, vol. 11, no. s2, Aug. 2013, Art. ID. S20604.